single grating embedded in an etalon. For proof-of-concept, we again chose $LiNbO_3$ again. Figure 4 shows the output passband spectrum of a single grating in etalon. In this case, multiple passes were achieved by two external mirrors (R1 ≅ 90%, R2 ≅ 99%) because of our present lack of facet-coating capability. The variation of the measured diffraction efficiencies over the wavelength range is consistent with the mirrors' loss and that of the crystal facets.

1. V. Minier and J.M. Xu, Opt. Eng. **32**, 2054 (1993).
2. J. Bismuth, A. Othonos, M. Sweeny, A. Kévorkian, J.M. Xu, in *Conference on Lasers and Electro-Optics*, Vol. 9, OSA Technical Digest Series (Optical Society of America, Washington, D.C., 1996), p. 513.

WL50

Phenomenological model of the integrated multifrequency laser

S.K. Shin, H. Kim, C.R. Giles,* M. Zirngibl,* Y.C. Chung,
Korea Advanced Institute of Science and Technology, Department of Electrical Engineering, Kusong-dong, Yusong-gu, Taejon 305-701, Korea; E-mail: ychung@eekaist.kaist.ac.kr

Recently, the integrated multifrequency laser (MFL) has been proposed for use as the central-office transmitter in wavelength-division multiplexing (WDM) access networks.[1] The MFL, consisting of a waveguide-grating router (WGR), individual channel amplifiers, and a common amplifier, is capable of emitting several different wavelength channels simultaneously into single fiber. Although the MFL is attractive as the channel spacing is precisely determined from the WGR, the output powers of the channel are interdependent because of the common intracavity amplifier, causing cross talk among the channels during modulation.[2] In this paper, we examine the output characteristics of the MFL from which we derive a simple phenomenological model to describe the cross talk-induced change in threshold and slope efficiency of each channel of the MFL. While it is not a dynamical model, it is still applicable at modulation rates below 1 Gbit/sec, which are typical for access networks. With this model, the MFL can be well characterized by a few simple measurements, enabling systematic device evaluation and better WDM transmitter design to include methods of cross talk reduction.

The MFL studied here consists of a WGR in InP with an array of eight multiple quantum well semiconductor amplifiers on one side and a common amplifier on the other. The channel spacing and free-spectral range of these eight-channel devices were approximately 80 GHz and 640 GHz, respectively. Data to develop the phenomenological model were obtained by measuring the L-I characteristics of the MFL with two simultaneously operating channels (channel 1 and channel 3). The experimental setup in Fig. 1 shows the output of the MFL was sent either directly to a power meter for total power measurements or to a planner silca flat-band WGR having 200-GHz channel spacing and 1600-GHz FSR to measure the power in each channel (including cases where channels emitted at two wavelengths, separated by the free-spectral range of the MFL, 640 GHz).

Model parameters were extracted from measurement of the total output power as shown in the contour plot of Fig. 2 for the case of the common output amplifier current, I_c = 70 mA and the MFL temperature, T_{mfl} = 17°C. The single-channel L-I curves lie along the x and y axes of the plot. The distinct breaks in Fig. 2 correspond to the threshold currents for the two channels, which increase with increased output

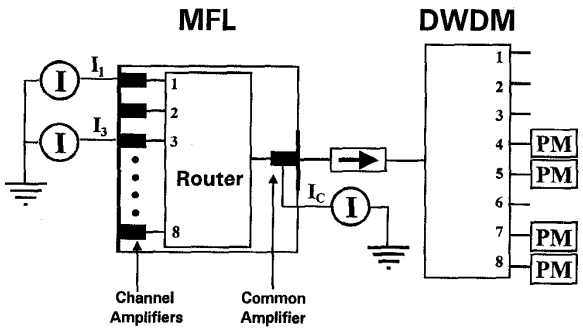

WL50 Fig. 1. Experimental setup to measure the L-I characteristics of the MFL. I are current sources and PM are optical power meters. DWMD is a planar silica waveguide grating router.

power of the interfering channels, as indicated in Fig. 2. Thus, the optical power, P_i, and threshold current, I_{thi}, of a channel i can be described phenomenologically by

$$P_i = \left(A_i - \sum_{j \neq i} B_{ij} P_j\right)(C_i - I_i)(I_i - I_{thi})$$

$$I_{thi} = I_{thoi} + \sum_{j \neq i} D_{ij} P_j,$$

where I_{thoi} is the threshold current of channel i when all other channels are turned off. The coefficients A_i and C_i, together with I_{thoi} describe the single-channel L-I curves, including a second-order output saturation caused by loss in the intra-cavity WGR. The coefficients B_{ij} result from sharing the output power of the common amplifier and D_{ij} characterizes the increase in threshold due to cross talk. These parameters are also

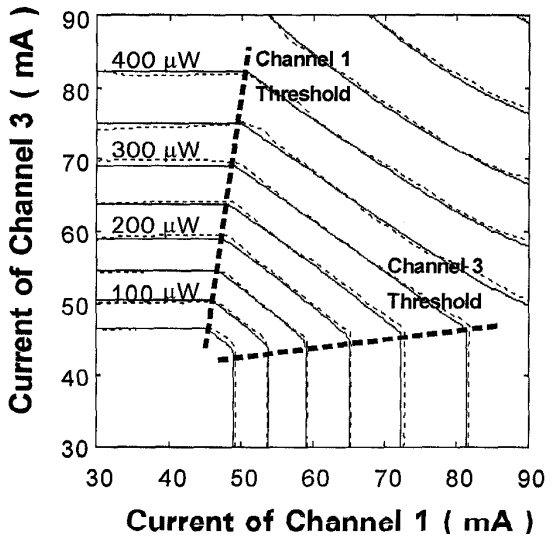

WL50 Fig. 2. Contour plot of the total output power of the MFL measured as a function of operating current of channels 1 and 3 on simultaneously. The dotted lines correspond to measured data and the solid lines are theoretically calculated using this model. Coefficients for this data were; $A_1 = 0.098$, $B_{12} = 8.4 \times 10^{-5}$, $C_1 = 164.61$, $D_{13} = 1.51 \times 10^{-2}$, $I_{tho1} = 44.62$ mA, $A_3 = 0.103$, $B_{31} = 8.4 \times 10^{-5}$, $C_3 = 181$, $D_{31} = 1.23 \times 10^{-2}$ and $I_{tho3} = 43$ mA. The optical power was measured in microwatts throughout this experiment.

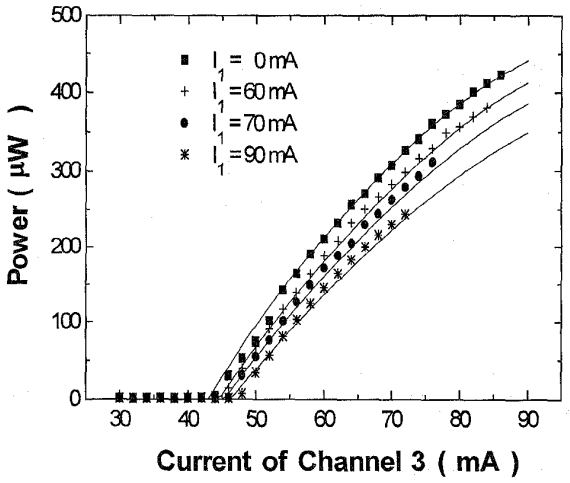

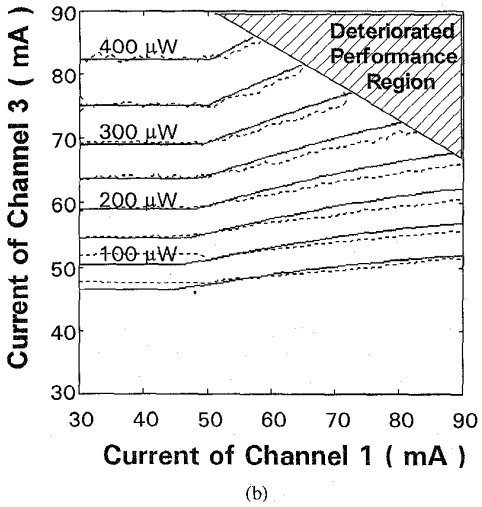

WL50 Fig. 3. Measured L-I curves of channel 3 in comparison to theoretically calculated curves (solid lines); (a) in an x-y plot, (b) in a contour plot. In these measurements, channels 1 and 3 operated simultaneously.

obtained from Fig. 2. The solid lines in Fig. 2 show values calculated using this model, which agree well with the measured data. Note that if all channels behaved identically, the MFL would be completely characterized by only five parameters, I_{tho}, A, B, C, and D.

To further test this model, the optical powers of each channel were measured separately, as shown in Fig. 1. Figure 3 shows the measured optical power of channel 3 with both it and channel 1 tuned on. The solid lines represent the calculated values using the model described above. The model was also successfully tested with three channels on simultaneously. Thus, we find that using this model, it would be possible to predict the L-I characteristics of each channel in the presence of cross talk, simply by measuring the total output power from the MFL.

In summary, we report a simple phenomenological model to describe the output characteristics of the MFL. The coefficients needed for this model are easily obtained by measuring the total optical power from every channel at the output of the MFL over the range of operating currents for each channel. The model could be used for device evaluation, performance monitoring, and improved transmitter design.

*Lucent Technologies, Bell Labs, 791 Holmdel-Keyport Rd, Holmdel, New Jersey 07733

1. M. Zirngibl, C.H. Joyner, L.W. Stulz, Electron. Lett. **30**, 1484–1485 (1994).
2. C.R. Doerr, C.H. Joyner, M. Zirngibl, L.W. Stulz, H.M. Presby, IEEE Photon. Technol. Lett. **7**, 1131–1133 (1995).

WL51

Step-tunable, all-optical wavelength conversion using cavity-enhanced four-wave mixing

J.A. Hudgings, K.Y. Lau, *Department of Electrical Engineering and Computer Science, University of California at Berkeley, Cory Hall, Berkeley, California 94720-1772; E-mail: jah@cory.eecs.berkeley.edu*

All-optical wavelength converters are key elements for wavelength-division multiplexing (WDM) optical communications systems, due to the need for reuse of the limited number of available carrier wavelengths. Wavelength converters based on four-wave mixing (FWM) in traveling wave amplifiers are being developed for use in systems that require transparency to modulation format. These devices are continuously tunable over a THz range, but the efficiency decays rapidly for conversion distances exceeding a few GHz.[1]

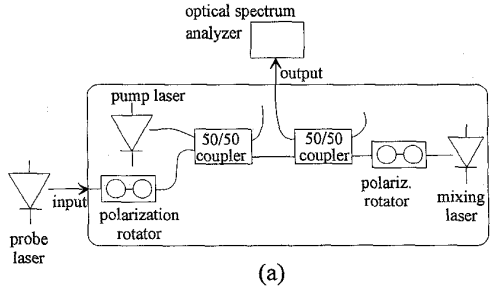

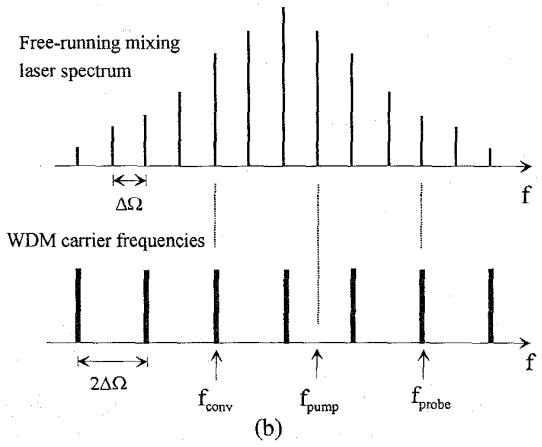

WL51 Fig. 1. (a) Wavelength conversion device; (b) Tuning the wavelength converter: given the desired input carrier frequency f_{probe} and desired converted output frequency f_{conv}, the device must be injection-locked into the mode at $f_{pump} = (f_{probe} + f_{conv})/2$.